

PARAMETERS OF DISKS AROUND YOUNG STELLAR OBJECTS FROM POLARIZATION OBSERVATIONS

PIERRE BASTIEN AND FRANÇOIS MÉNARD

Observatoire du Mont Mégantic, and Département de Physique, Université de Montréal

Received 1990 January 2; accepted 1990 May 18

ABSTRACT

Linear polarization maps of young stellar objects in which a pattern of aligned polarization vectors are observed close to the central object have been interpreted recently in terms of multiple scattering in flattened, optically thick, structures (Bastien and Ménard). These patterns provide *direct* evidence for circumstellar disks around young stellar objects. Circular polarization, which is predicted by this model, has been detected in a few stars already; however, it cannot be accounted for by a competing suggestion in which the pattern of aligned vectors is due to dichroic extinction by aligned nonspherical grains. This fact and many other objections lead us to reject aligned grains as a suitable model for the observations. In this paper, we use the results of the Bastien and Ménard model calculations to derive some parameters which represent best the observations. In particular, the size of the optically thick part of the disks, and their inclination to our line of sight is determined for published polarization maps. The distribution of inclination angles is consistent with the expected distribution. Inclination angles and disk sizes compare well with values obtained by other methods for the objects in common.

Subject headings: interstellar: grains — polarization — stars: circumstellar shells — stars: pre-main-sequence

I. INTRODUCTION

Many linear polarization maps of young stellar objects (YSOs) have been published in the past few years. In these maps, the polarization vectors are usually perpendicular to the radius vector from the central illuminating source. Such a centrosymmetric pattern is typical of reflection nebulae where single scattering is responsible for the polarization since the polarization vectors are usually perpendicular to the scattering plane.

However, departure from this single scattering pattern is clearly seen in regions close to the central star in $\sim 60\%$ of the objects (see Bastien and Ménard 1988, hereafter BM, and Table 1). In this region the polarization vectors are roughly perpendicular to the symmetry axis of the bipolar nebula, i.e., parallel to an equatorial disk structure. Until recently, these patterns of aligned polarization vectors were usually interpreted e.g., Warren-Smith, Draper and Scarrott 1987b, Warren-Smith 1987) as due to dichroic extinction by elongated grains aligned by a toroidal magnetic field, this toroidal field being the remnant of the gravitational collapse of a molecular cloud with a frozen-in magnetic field (e.g., Mestel and Paris 1984).

However, BM have proposed recently an alternative way to produce patterns of aligned polarization vectors in YSOs. Their mechanism makes no assumption whatsoever about the grain size and shape and requires no magnetic field. The only requirements concern the geometry of the bipolar nebula itself. While the bipolar lobes may be optically thin, the equatorial disk should be optically thick. This is precisely the geometry generally adopted for many YSOs. Single scattering in the optically thin lobes naturally gives a centrosymmetric pattern while the large optical depth in the equatorial disk ensures multiple scattering. This multiply scattered light is, according to the BM model, the key factor for producing bands of aligned polarization vectors in YSOs. Indeed, consideration of double scattering only is sufficient to explain published polarization maps (BM).

We first consider the observed characteristics of polarization maps (§ II), then examine critically the competing models for their interpretation (§ III) to conclude that multiple scattering is the dominant process. On the basis of the BM model, we deduce (§ IV) inclination angles and disk sizes, and compare (§ V) these values with information obtained by other methods.

II. BASIC CHARACTERISTICS OF POLARIZATION MAPS

Optical and near-IR linear polarization maps which have been published so far are listed in Table 1. Only galactic sources are considered in this table, although maps of many extragalactic objects have been obtained. These sources include one or two young planetary nebula (M2-9, IRAS 07131-0147) and a cataclysmic variable (η Car); all other sources are confirmed or probable YSO's. The polarization patterns are classified in column (2) into centrosymmetric (cs), aligned vectors (av), and peculiar (pec). The third column gives the central wavelengths of the bandpasses used for obtaining the maps; column (4) answers the question: Is the central source visible? The resolution at which the maps have been taken is given in column (5). If aligned vectors are visible in at least part of the map, the object is assigned to the "av" category, even though the polarization vectors are centrosymmetric in the rest of the map. Here we note that if the observations are repeated with improved spatial resolution, some objects with a centrosymmetric pattern may eventually show a pattern of aligned vectors close to the central source.

We now discuss the basic characteristics of linear polarization maps. Successful models have to account properly for these characteristics. We consider a map with a pattern of aligned linear polarization vectors, since it contains all the features that we want to examine. Those which are centrosymmetric can be considered as lacking some of the characteristics described below.

1. An extended centrosymmetric pattern. By taking perpendiculars to each vector, the position of the central source can be determined. In some cases, this centrosymmetric pattern is

altered near the edge of the bipolar region, good examples of this property are found in the polarization maps of R Mon (Scarrott, Draper, and Warren-Smith 1989), and PV Cep (Gledhill, Warren-Smith, and Scarrott 1987).

2. A pattern of aligned vectors close to the central source. The vectors can be either well aligned or, as in many cases, form an elliptical rather than centrosymmetric pattern. The polarization in this region is typically 10%–15%. In one object, V645 Cyg, it reaches 30% (Lenzen 1987a).

3. Polarization null points. In the region of aligned vectors, as one goes further away from the source, the vectors rotate to become perpendicular to the disk, or equivalently, centrosymmetric again. In between, the polarization goes to zero. The two points on either side of the central source where this happens have been termed “null points” by Scarrott, Draper, and Warren-Smith (1989).

In addition to these features of the linear polarization maps, the models also have to explain the other polarization properties of T Tauri stars and other young stellar objects. A detailed review of these properties, and models to account for them, was given by Bastien (1988b).

III. THE INTERPRETATION OF LINEAR POLARIZATION MAPS

The explanation for the centrosymmetric pattern in terms of single scattering by dust grains is generally accepted. The high levels of polarization, reaching sometimes up to $\approx 70\%$, which have been observed are well accounted for by single scattering. Small grains are required to explain the largest observed polarization levels. Such polarization patterns are the signature of reflection nebulae. Therefore, the linear polarization in the usually bipolar, and sometimes monopolar, nebulae typical of YSOs are well explained.

However, the explanation of the patterns of aligned vectors close to the central source has not been unanimous. Here we

discuss the various mechanisms which have been proposed so far.

a) Dichroic Extinction

Dichroic extinction by aligned nonspherical grains in a circumstellar disk has been proposed by many authors. While various alignment mechanisms are possible, alignment by a toroidal magnetic field is usually preferred. We note that no model calculations of aligned grains have been performed. Only arguments of a qualitative nature, related to interstellar polarization, have been invoked.

There are many arguments which can be raised against aligned grains for explaining the patterns of aligned vectors:

1. The high level of polarization, typically 10%–15%, reaching up to 30%, observed in regions where the polarization vectors are aligned requires very efficient grain alignment, which is not understood.

2. The wavelength dependence of linear polarization does not follow the smooth interstellar polarization law, found by Serkowski (1973) and expected for aligned grains. On the contrary, a great variety of wavelength dependencies have been observed, and they cannot be accounted for by aligned grains.

3. The polarization reversal, i.e., rotation of the plane of polarization by 90° , from the visible to the near-infrared in T Tau and possibly also in SU Aur (Hough *et al.* 1981), cannot be reproduced with aligned grains.

4. The correlations in the temporal variations of polarization with the light curve in B and V for the star RY Lup (Bastien *et al.* 1989, unpublished observations) are incompatible with dichroic extinction. Most likely, similar correlations exist for other young stars.

5. The large, i.e., $\Delta P \geq 1\%$ and/or $\Delta\theta \geq 30^\circ$, and rapid, i.e., $\Delta t \leq 1\text{--}3$ days, polarization variations observed in many T Tauri stars (e.g., Bastien 1985; Drissen, Bastien, and St-Louis

TABLE 1
POLARIZATION MAPS OF GALACTIC SOURCES

Object (1)	Polarization Pattern (2)	λ (μm) (3)	Central Source Visible (4)	Resolution ($''$) (5)	References (6)
NS 3	cs	0.85	yes	3.6	1
W3 IRS 1, 2	av	2.2	IR	7	2
FS Tau (Haro 6-5)	av	0.65	yes	2.5	3, 4, 5
	av	0.65	yes	1.25	6
Haro 6-5B	av	0.65	yes?	2.5	3, 4, 5
	av	0.65	yes?	1.25	6
LkH α 101/NGC 1579	cs	0.52, 0.75	yes	6	7
	cs	2.2	yes	8	7
	cs	0.65	yes	5	8
L1551 IRS 5	cs*	0.8	IR	*	9
	av	0.75	IR	13	4, 5, 10
	av	≈ 1.0	IR	0.9	11
	av	0.67	IR	0.5	12
L1551 NE	av?	0.75	IR	13	4, 5, 10
LkH α 358	av	0.75	yes	≈ 1	6
HL Tau	av	0.75	yes	1.25	6
XZ Tau	pec*	0.75	yes	1.25	6
BN/KL	av	2.2	IR	2.5	13
	*	3.8	IR	*	14
	av	2.2	IR	1	15
IRAS 05329-0505	av	0.8	yes	7.2	16
HH 34 IRS	av?	0.67	yes	0.75	17
HH 34 Bipolar Nebula	av	0.67	yes	1	17
HH 34 IRS 5 Nebula	pec*	0.67	IR	1.25	17
VLA1/HH 1,2/NGC 1999	*	0.78	IR*	*	18
	av*	0.8	IR*	5	5

TABLE 1—Continued

Object (1)	Polarization Pattern (2)	λ (μm) (3)	Central Source Visible (4)	Resolution ($''$) (5)	References (6)
V380 Ori	cs	0.55	yes	5	19
Re 50 IRS/IRAS 053338-0728	pec*	0.75	no	1.75	20
SSV 63/HH 24	av	0.75	IR	4	21
SSCV 140	cs	0.75	yes	4	21
LkH α 304/S 108	cs	0.67	yes	3.5	22
	av	0.78	yes	3.5	22
Horsehead Nebula/B 33	pec*	0.72	—	10.8	23
	pec	0.85	—	—	24
NGC 2071 IR	pec	2.2	IR	6	2
LkH α 208	cs	0.55	yes	5	25
R Mon/NGC 2261	av	0.46, 0.5, 0.75	yes	6	7
	—	2.2	yes	—	7
	av	0.52, 0.65	yes	5	26
	av	0.46	yes	0.76	27
	av	*	yes	*	28
	av	0.65	yes	6	29
GL 989/NGC 2264 IR	av?	2.2	IR	4	2
	cs*	0.65	no	1.25	30
NS 14	av	0.85	IR?	3.6	1
IRAS 07131-0147	av	0.65	yes	2.5	31
OH 0739-14	av*	2.2	IR	3	32
HH 46 IRS	av	0.75	yes	0.5	33
η Car	av	0.55	yes	0.7	34
Cha IR Nebula	av	0.75	*	≈ 3	35
Bruck "Bipolar Nebula"	pec*	0.75	*	3	36
GSS 30	cs	2.2	IR	1.5	37
HH 57 IRS	cs	0.75	IR(yes?)	1.5	38
M 2-9	av	0.76	yes*	0.74	39
NGC 6334 IRS V	pec*	0.75*	—	1.6	40
M 8 Hourglass	—	0.52	no	3.5	7
	cs?	0.74	no	3.5	7
	—	2.2	no	≈ 10	7
GGD 27 IRS	cs	2.2	IR	15	41, 42
	cs	3.8	IR	*	41
Serpens Nebula	av	0.65	yes	4	43
	av	0.55	yes	1	43
	av	0.78	yes	2.5	44
	av	0.78	yes	4	44, 45
	av	*	yes	2.5	44
HH 100	av*	0.75	no	3.5	44
R CrA	av	0.65	yes	1	47
T CrA	av	0.65	yes	1	47
Parsamyan 21	av	0.85	yes	3.6	48
S 100	*	0.52	*	3.3	7
	*	2.2	*	—	7
LkH α 225	—*	2.2	yes	*	7
S 106	cs	2.2	yes	6	7
	cs	2.2	yes	*	49
	pec	0.8	yes	6	50
	cs	0.4	yes	6	50
	cs	0.76	yes	2	51
GL 2591	cs	≈ 1.0	IR?	≈ 0.9	11, 52
	cs	2.2	IR	20	53
	cs	2.2	IR	10	54
	cs	1.65	IR	2	55
	cs	2.2	IR	2	55
	av	0.75	no*	2.5	56
W75N	pec*	2.2	IR?	15	57, 41
PV Cep	av	0.78	yes	2.5	5
	av	0.75	yes	4	58
	av	0.78	yes	4	58
V645 Cyg (GL 2789)	av	2.2	yes	*	7
	av	1.0	yes	≈ 0.9	11
NGC 7129 (RNO 138)	cs	0.85	*	3.6	59
S140 IRS (GL 2884)	cs	2.2	IR	20 \times 30	60
	av*	1.0	IR	0.9	11
LkH α 233	av	0.55	yes	0.5*	61
Cep A/GGD 37	cs	2.2	no	20	59
	cs	3.6	no	*	62
S158 IRS 4	pec*	2.2	IR*	3	2

TABLE 1—Continued

^a Meaning of abbreviations: cs, centrosymmetric; av, aligned vectors; pec, peculiar, refer to notes on individual sources; asterisk, see notes on individual sources.

^b In this column, IR means that the source is detected in the infrared only, not at visible wavelengths.

NOTES.—NS 3: Scarrott *et al.* 1986a proposed aligned vectors.

W3 IRS 1, 2: av if IRS 2 is the central object, which is what Heckert and Zeilik 1984 assumed.

Haro 6-5B: The isophotes are stellarlike.

LkH α 101: The H II region around NGC 1579 is also known as S 222. The polarization measured in the wide passbands used by Lacasse (1983) are most likely diluted by the strong emission from the H II region. He also made a 5 point polarization map at 2.2 μ m which is consistent with a centrosymmetric pattern even with the large errors.

L1551 IRS 5: The scale is not given by Stocke *et al.* 1988, the map covers the whole nebula, but only with a few vectors. The cs pattern is therefore due only to the poor spatial resolution.

L1551 NE: The flux is too low on the source because of high extinction, therefore one cannot be sure about the pattern type.

XZ Tau: There is no evidence for nebulosity around this star, according to Gledhill and Scarrott 1989.

BN/KL: OMC-1 which contains the Becklin-Neugebauer/Kleinmann-Low infrared region is quite complex. Near IRC2, Hough *et al.* 1986 favor superparamagnetic grains or grains aligned by a magnetic field larger than in the general interstellar medium to explain the polarization pattern in the molecular hydrogen emission line at 2.2 mm. They suggest that this mechanism is dominated by scattering at 3.8 mm. The 3.8 mm map is not on a square grid, the vectors are spaced by 5" to 10" and are aligned between BN and IRC 2.

HH 34 IRS: There is a stellar-like peak in the isophotes; if it is not the central source, then av should be changed.

HH 34 IRS 5 Nebula: The pattern does not include the source whose identification is uncertain.

VLA1/HH 1.2/NGC 1999: Strom *et al.* 1985 gave a map with only a few polarization vectors. The illuminating source is probably NGC 1999 IRS 2 according to Scarrott *et al.* 1986b; if not, av should be changed.

Re 50 IRS/IRAS 053338-0728: There are two nebulae about 80" apart and Scarrott and Wolstencroft 1988 suggest that they are both illuminated by an unknown and undetected source exterior to both nebulae.

LkH α 304/S 108: In the R band, the source is HD 37903, but in the I band, the source is LkH α 304 which modifies the pattern locally.

Horsehead Nebula/B33: This region is illuminated by a distant star, σ Ori. Warren-Smith, Gledhill, and Scarrott 1985 also suggest the possible presence of aligned grains to explain their map.

NGC 2071 IR: The 2.2 mm map is consistent with a scattering mechanism. However, the map is not extended sufficiently to give it a definite pattern.

R Mon: There is a hint of aligned vectors in the low-spatial resolution ($\approx 6''$) maps by Lacasse 1983. Ten maps taken by Scarrott and coll. during the period 1979–1985 have been put together in Scarrott, Draper, and Warren-Smith 1989.

GL 989/NGC 2264 IR: There are only a few vectors in the 2.2 μ m map. GL 989 is not the illuminating source as proposed by Scarrott and Warren-Smith 1989. The pattern is cs around an undetected source.

IRAS 07131-0147: Wolstencroft, Scarrott, and Menzies 1988 suggest that this source is a protoplanetary nebula.

OH 0739-14: The map is too small, care is therefore required.

η Car: This is a cataclysmic variable.

Cha IR Nebula: The position of the IR source is shifted slightly with respect to the pattern of aligned vectors.

Bruck "Bipolar Nebula": This is not really a bipolar nebula, but there are two sources illuminating the same nebula.

GSS 30: Castelaz *et al.* 1985 suggest that $i \geq 65^\circ$, in which case the pattern should be av. This object should be mapped again.

M2-9: This is a young planetary nebula.

NGC 6334 IRS V: This is a complex region with many possible sources. It requires observations with higher spatial resolution.

M 8-Hourglass: There are three stars close to this bipolar nebula.

GGD 27 IRS: The 3.8 μ m map is not on a square grid and many sources are present.

Serpens Nebula: Warren-Smith, Draper, and Scarrott 1987b present 4 small maps in the bands: V, R, I, and Z.

HH 100: If HH 100 IRS is the source, the pattern should be classified pec instead of av.

S100: There is a compact H II region, K3-50, which appears starlike at visible wavelengths. The object is covered by uniform polarization vectors aligned north-south. The illuminating star, which must be outside the region, has not been identified.

LkH α 225: Only seven positions including the star have been measured. It is therefore impossible to assign this object to a specific group.

S 106: The map by McLean *et al.* 1987 is not on a square grid.

GL 2591: The IR source in the other papers is not the illuminating source at 0.75 μ m for this object as shown by the map by Rolph and Scarrott 1988.

W75N: A very complicated field.

V645 Cyg (GL 2789): Not a square grid Lacasse 1983.

NGC 7129 (RNO 138): The source seems to be the peak in the isophotes in the nebula rather than the nearby star.

S140 IRS (GL 2884): There are three IR sources in this region (Lenzen 1987a). IRS 3 has a cs pattern and IRS 1 an av pattern.

LkH α 233: The seeing was 1".5.

Cep A/GGD 37: The 3.6 μ m map is not on a square grid, the resolution is too low.

S158 IRS 4: This object, in NGC 7538, is probably a polarized reflection nebula illuminated by S158 IRS 5, a special case of a scattering mechanism with the exciting star not embedded in the nebula (Heckert and Zeilik 1984). If the source is IRS 4 instead of IRS 5, the pattern should be av.

REFERENCES.—(1) Scarrott *et al.* 1986a; (2) Heckert and Zeilik 1984; (3) Gledhill, Warren-Smith, and Scarrott 1986; (4) Scarrott *et al.* 1985; (5) Scarrott *et al.* 1986b; (6) Gledhill and Scarrott 1989; (7) Lacasse 1983; (8) Redman *et al.* 1986; (9) Stocke *et al.* 1988; (10) Draper, Warren-Smith, and Scarrott 1985c; (11) Lenzen 1987a; (12) Scarrott 1988a; (13) Hough *et al.* 1986; (14) Werner, Dinerstein, and Capps 1983; (15) Aspin 1988; (16) Wolstencroft *et al.* 1986; (17) Scarrott 1988b; (18) Strom *et al.* 1985; (19) Warren-Smith *et al.* 1980; (20) Scarrott and Wolstencroft 1988; (21) Scarrott, Gledhill, and Warren-Smith 1987b; (22) Scarrott, Rolph, and Mannion 1989; (23) Zaritsky *et al.* 1987; (24) Warren-Smith, Gledhill, and Scarrott 1985; (25) Shirt, Warren-Smith, and Scarrott 1983; (26) Gething *et al.* 1982; (27) Aspin, McLean, and Coyne 1985; (28) Scarrott, Draper, and Warren-Smith 1989; (29) Warren-Smith, Draper and Scarrott 1987a; (30) Scarrott and Warren-Smith 1989; (31) Wolstencroft, Scarrott, and Menzies 1988; (32) Heckert and Zeilik 1983; (33) Scarrott and Warren-Smith 1988; (34) Warren-Smith *et al.* 1979; (35) Scarrott *et al.* 1987a; (36) Scarrott *et al.* 1987b; (37) Castelaz *et al.* 1985; (38) Scarrott, Gledhill, and Warren-Smith 1987a; (39) Aspin and McLean 1984; (40) Wolstencroft, Scarrott, and Warren-Smith 1987; (41) Yamashita *et al.* 1987b; (42) Nagata *et al.* 1987; (43) King, Scarrott, and Taylor 1983; (44) Warren-Smith, Draper, and Scarrott 1987b; (45) Warren-Smith, Draper, and Scarrott 1987c; (46) Scarrott *et al.* 1987c; (47) Ward-Thompson *et al.* 1985; (48) Draper, Warren-Smith, and Scarrott 1985a; (49) McLean *et al.* 1987; (50) Lacasse *et al.* 1981; (51) Aspin *et al.* 1989; (52) Lenzen 1987b; (53) Yamashita *et al.* 1987a; (54) Hodapp 1984; (55) Burns *et al.* 1989; (56) Rolph and Scarrott 1988; (57) Yamashita *et al.* 1988; (58) Gledhill, Warren-Smith, and Scarrott 1987; (59) Draper, Warren-Smith, and Scarrott 1985b; (60) Joyce and Simon 1986; (61) Aspin, McLean, and McCaughrean 1985; (62) Lenzen, Hodapp, and Solf 1984.

1989) would require changing grain alignment on very short time scales. Even slower, $\Delta t \approx$ a few months, but large polarization variations (from 1% to $\approx 8\%$ and back to $\approx 1\%$), such as happened in the T Tauri star UY Aur (Ménard and Bastien 1987), would be difficult to explain with aligned grains.

6. Circular polarization which has been detected in three T Tauri stars, RY Tau, T Tau, and SU Aur (Nadeau and Bastien 1986; Bastien, Robert, and Nadeau 1989) cannot be explained by aligned grains simultaneously with the pattern of aligned linear polarization vectors. Circular polarization has also been detected in that part of the nebulosity where the linear polarization vectors are aligned, which corresponds to the disk near R Mon; however, it was not detected in the lobes, where only single scattering is present (Ménard, Bastien, and Robert 1988). Again, these detections are incompatible with dichroic extinction.

7. The null points cannot be explained by dichroic extinction alone; Scarrott, Draper, and Warren-Smith (1989) had to invoke another mechanism in addition to aligned grains.

b) Multiple Scattering

All the above arguments against dichroic extinction are well explained by models with single and multiple scattering in optically thick circumstellar disks:

1. Polarization reaching $\approx 20\%$ in the region with aligned polarization vectors is typical in the results of Monte Carlo calculations (Ménard 1989; Ménard and Bastien 1990). In § IV we use the results of the BM model to deduce the size and the inclination of the optically thick disks from published polarization maps.

2. A great variety of wavelength dependencies can be obtained with scattering by dust grains; there are many parameters that can be changed to fit the observations: the size, chemical composition, and spatial distribution of the grains.

3. The polarization reversal poses no problem with scattering: a reduction in optical depth, which is expected, in going from short to long wavelengths will rotate the position angle by 90° . Other possibilities have also been discussed by Bastien (1987); from the evidence currently available, these appear less likely than the variation in optical depth with wavelength.

4. The correlations between polarization and the light curve in B and V can be explained by changing the way that the grains are illuminated. For example, a spot on the star will change the light curve in a periodic manner and this periodicity will also be reflected in the polarization.

5. The rapid polarization variations can be explained by nonisotropic changes in stellar brightness, e.g. a flare or spots on the surface. These phenomena are thought to be common on these stars.

6. Circular polarization is well explained by multiple scattering. It was in fact first predicted from the BM model (see Bastien 1988a) and later confirmed by observing R Mon (Ménard, Bastien, and Robert 1988). Similarly, the circular polarization detected in three T Tauri stars is due to multiple scattering (Bastien, Robert, and Nadeau 1989).

7. The null points find also an easy explanation with scattering: far from the source, the polarization pattern becomes centrosymmetric again because the amount of material available decreases, hence also the optical depth.

c) Other Explanations

Notni (1985) proposed an alternative way to produce an elliptical pattern close to the central source, in the context of

galaxies. He *assumed* that the central source is already strongly linearly polarized, and then computed analytically the ellipticity of the polarization pattern due to single scattering in the reflection nebula. However, the assumption that the source is already polarized is unnecessary in the BM model. Notni's results support, nevertheless, the BM model.

IV. DISK PARAMETERS

Now, we use the polarization maps computed with the *ad hoc* model presented by BM to estimate some parameters of the disks. This model treats scattering according to the Mie theory for perfect spherical grains. However, the location of the scatterers is not free in the model: the position of the scatterers is specified explicitly. Rigorous Monte Carlo calculations in which this restriction is relaxed have already been performed (Ménard 1989, Ménard and Bastien 1990) and confirm the results of the *ad hoc* model. Here we use the BM model for convenience, and note that our conclusions are not affected by its simplifying assumptions.

For future reference and so that other workers may also estimate the inclination angle of polarization maps, we present in Figure 1 maps computed with the BM model for a grid of inclination angles, from 90° to 50° in steps of 5° . These calculations have been performed for silicate grains with a radius of $0.1 \mu\text{m}$ and at a wavelength of $0.5 \mu\text{m}$.

The extent of the optically thick part of the disks and their inclination to the line of sight can be determined for the objects where aligned vectors are observed. Table 2 gives for those objects the inclination (col. [2]) as determined from a direct comparison of the observed vector patterns with our model calculations (Fig. 1). The observed sizes (col. [3]) of aligned vector areas in the polarization maps give directly the size of the disks, or more precisely, the size of the area where the optical depth at the wavelength of the observation is ≥ 1 . The observed sizes (col. [3]) can be used to estimate the minor to major axes ratio (col. [4]) of the disks. From this ratio, another value of the inclination (col. [5]) can be computed. The inclination from the second method (col. [5]) is less reliable because of observational problems, e.g., the region with aligned vectors extends up to the edge of the maps, or poor spatial resolution. The first value of the inclination (col. [2]) is therefore to be preferred in case of disagreements between the two methods.

There are no values of inclination less than 50° in Table 2 because the model yields a nearly centrosymmetric pattern for inclinations less than $\sim 40^\circ$.

In order to allow another way to get an idea about the model and results we derive from it, we present in Figure 2 a direct comparison between the model and observations for Parsamyan 21. From Table 2, the inclination we derived for this object is close to 90° , which resembles the BM map for an edge-on disk.

The spherical grain hypothesis does not affect the results, especially the inclination. In fact, the inclination given in column (5) is independent of the model as it comes directly from the axis ratio in the maps. Any possible error is therefore due only to the observational problems mentioned above. The first method (column 2) has an error of $\sim 5^\circ$, the difference in the inclination between two maps. For both methods, the spatial resolution is very critical for evaluating the inclination. We think that our values of inclination are typically accurate to 5° – 10° ; however, there may be some exceptions due to the observational limitations mentioned above.

It is difficult to estimate the error associated with the assumed disk shape in the BM model as it does not lend itself

TABLE 2
DISKS PARAMETERS FROM LINEAR POLARIZATION DATA

Object (1)	i^a degree (2)	Size ^b (" × ") (3)	Ratio ^c (4)	i^d degree (5)
W3 IRS 1, 2	...	28 × 28
FS Tau (Haro 6-5)	60	6 × 4	0.61	52?
Haro 6-5B	≈ 60	≈ 10 × ≈ 20	≈ 0.5	60
L1551 IRS 5	> 80	≈ 70 × ≈ 15	0.15	81
L1551 NE
LkHα 358	...	4.5 × 2	0.45	≈ 65
HL Tau	70	≈ 7 × 3	0.43	≈ 65
BN	70–75	≈ 15 × ≈ 5	≈ 0.3	72
IRAS 05329-0505	75–80	10 × 20	0.25	75
HH 34 IRS	...	15 × 10	0.66	50?
HH 34 Bipolar Nebula	...	> 5 × 25	< 0.5	> 60
VLA 1/HH 1-2
SSV 63/HH 24	> 75	40 × 15	0.38	70
LkHα 304/S 108	> 80	15 × 10	0.66	50?
R Mon/NGC 2261	75–80	10 × 55	0.2	78
	75–80	10 × 40	0.25	75
GL 989/NGC 2264	50–60?	16 × 16
NS 14	55–60	10 × 20	0.5	60
IRAS 07131-0147	85–90	> 30 × 10	< 0.3	> 70
OH0739-14	< 60?	15 × 5
HH 46 IRS 5	80	≈ 7 × ≈ 2	≈ 0.3	≈ 75
η Car	> 60	≈ 5 × ≈ 3	≈ 0.6	≈ 55
Cha IR Nebula	85	9 × 18	0.5	60
M2-9	≈ 60–≈ 75	6 × 3	0.5	60
Serpens Nebula	75–80	40 × 10	0.25	75
HH 100	80–90	> 45 × ≈ 15	0.3	> 70
R CrA	50–60	8 × 14	≈ 0.5?	60
T CrA	85–90	≈ 10 × 20?	≈ 0.5?	60
Parsamyan 21	80–85	≈ 30 × ≈ 8	0.25	75
GL 2591	> 70	17.5 × 7.5	0.43	65
PV Cep	> 60	10 × 30	0.4	> 60?
V645 Cyg	60–70	10 × 5	0.5?	60?
S140 IRS (GL 2884)
LkHα 233	85–90	2 × 15	< 0.1	≈ 90

^a Inclination angle of the disks as determined from direct comparison with computed polarization maps.

^b Size in arcseconds of the observed area with aligned polarization vectors.

^c Aspect ratio of the observed area with aligned polarization vectors, assuming that it is complete and symmetric about the axis of symmetry of the bipolar nebula.

^d Inclination angle as determined from the aspect ratio in col. (4).

NOTES.—W3 IRS 1, 2: The angular resolution is not particularly good (7"). In addition, there are three IR sources within the area where aligned polarization vectors are observed. Additional data are required.

FS Tau, Haro 6-5B: Depending on the contribution of FS Tau (Haro 6-5), what we think to be aligned vectors near Haro 6-5B might well be centrosymmetric vectors around FS Tau (see map given by Scarrott *et al.* 1985).

L1551 IRS 5: The map of Draper *et al.* 1985c was used. It is difficult to get useful information from the map by Lenzen (1987a).

BN: Because of the proximity of the other sources, a better resolution is required to isolate the effect of the BN object alone. The size in col. (3), as determined from the *K* band map by Hough *et al.* (1986) is therefore subject to changes. The same authors show also a map in the molecular hydrogen band, with a well-defined region of aligned polarization vectors; its interpretation is also complicated by the same effect mentioned above.

HH 34 IRS: The *av* pattern extends to the edge of the map.

HH 1-2: A very complex region, which requires a higher spatial resolution.

LkHα 304/S 108: Nearby HD 37903 influences the pattern, making it difficult to make reliable estimates.

R Mon: The first line is deduced from the map by Warren-Smith, Draper, and Scarrott (1987a), while the second one is based on a map by Gething *et al.* (1982). On the Gething *et al.* map, aligned vectors are visible up to the limit of the map.

NGC 2264: One would like better resolution; all the vectors seem aligned.

NS 14: Aligned vectors are visible to the edge of the map.

OH 0739-14: There are not enough vectors and the resolution is too coarse. One should wait for better measurements because two sources are visible.

Chamaeleon IR Nebula: The aspect ratio is not reliable because the vectors

TABLE 3
POLARIMETRIC MODELS OF BIPOLAR NEBULAE

i deg. (1)	P_{\max} (lobe) % (2)	P_{\max} (disk) % (3)
45	54	28
50	54	19
55	55	17.5
60	54	19
65	57	14
70	80	10
75	95	8
80	94	8
85	75	11
90	60	9

NOTES.—The values above have been computed according to the following model: Physical parameters: $\lambda = 5000 \text{ \AA}$, grain radius: $a = 0.2 \text{ \mu m}$ grains of amorphous carbon ($m = 2.27-0.64i$).

Geometrical parameters: in non-dimensional units: the lobes are given by paraboloids: $z = 0.15(x^2 + y^2)$, circular disk with radius = 11, thickness = 3.

to test disk shapes other than flat ones. This problem is alleviated in the more realistic Monte Carlo model. Examination of results obtained so far with this later model with a small number of resolution elements show that the results obtained with the BM model are comparable for estimating inclination values. The same axis ratio for the region of aligned polarization vectors is obtained for both models at the same inclination angle. The shape of the disk in the Monte Carlo calculations was in fact convex; i.e., contours of equal density are convex. Therefore, it seems that the exact shape of the disk does not affect significantly the polarization pattern.

Table 3 gives, for one typical set of parameters, maximum values of the linear polarization in the lobes and in the disk for various inclination angles. The parameters specifying the model are also given. Maps for other grain compositions, radii, etc. can be easily computed. There are no large differences. The differences are in the level of polarization, not in the position angles which remain the same. Hence, the estimates of inclination angles (i.e., in Table 2) are not affected by such changes in our assumptions. Large values of polarization can be easily obtained in the lobes, in good agreement with the observa-

TABLE 2—Continued

are lined up to the edge of the map. The inclination as determined in column (2) is reliable.

Serpens Nebula: The results were determined from Fig. 3 of Warren-Smith, Draper, and Scarrott (1987b, 1987c). One of the best cases.

R CrA: The map does not extend far enough: aligned vectors are visible up to the edge of the map.

T CrA: Again, the map does not cover a large enough area. On the larger scale map of NGC 6729 there is a hint that aligned vectors are in fact centrosymmetric vectors around another source.

Parsamyan 21: A very nice case for illustrating the model (see Fig. 2).

PV Cep: The inclination is difficult to determine from the aspect ratio because one sees aligned vectors along the eastern edge of the northern lobe. This is not a centrosymmetric pattern, but this is also not a typical disk pattern. The values in cols. (4) and (5) have been obtained by cutting the extent of the "disk" arbitrarily.

V645 Cyg: The area with aligned vectors is almost entirely determined by the size and shape of the map.

S140 (GL 2884): The *av* pattern concerns IRS 1 only.

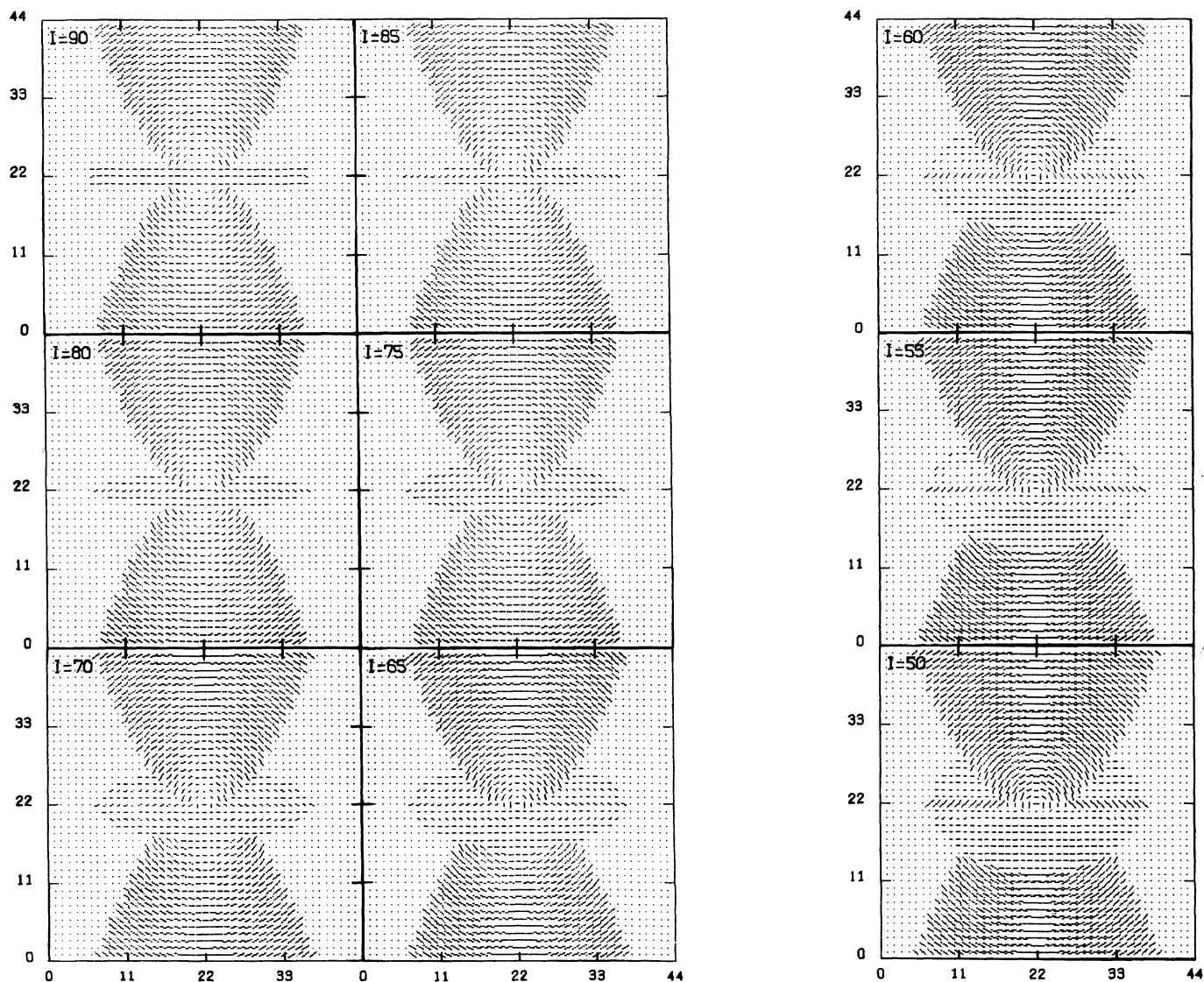


FIG. 1.—(a) and (b) A mosaic of polarization maps computed with the BM model for various values of the inclination angle, as indicated. The near edge of the inclined disks is toward the bottom of the figure. See text for more details.

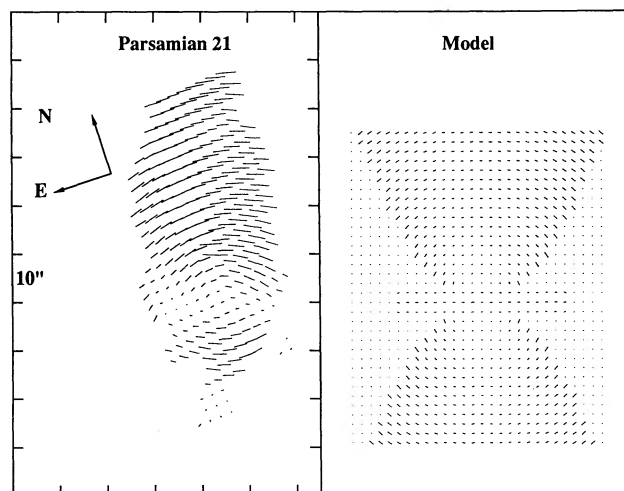


FIG. 2.—Comparison between the observed polarization map of Parsamian 21 (Draper, Warren-Smith, and Scarrott 1985a), and results from the BM model for a disk seen edge-on. The scale and orientation of the polarization map for Parsamian 21 are as indicated.

tions. Similarly, the polarization level reached in the disk compares quite well with the observations.

V. DISCUSSION

Comparison of our polarization model with observations has enabled us to infer values for the size and the inclination of the disks around YSOs. In this section, we compare the values we obtained with other estimates of these parameters in the literature, but first we examine the statistics of the distribution of inclination angles.

a) Statistics

In Figure 3, we show a histogram of the inclination angle distribution for the sources included in Table 1 and which have or are likely to have a circumstellar disk ($N = 49$). We leave out seven sources which belong to complex regions or whose illuminator lie outside the mapped area. These sources are: HH 34 IRS 5 Neb., Re 50 IRS, Horsehead Nebula, Bruck "Bipolar Nebula," S100, W75N, S158 IRS 4.

As mentioned above, sources with a centrosymmetric pattern have an inclination angle less than $\approx 50^\circ$ which cannot be determined more precisely. In Figure 3, these sources have

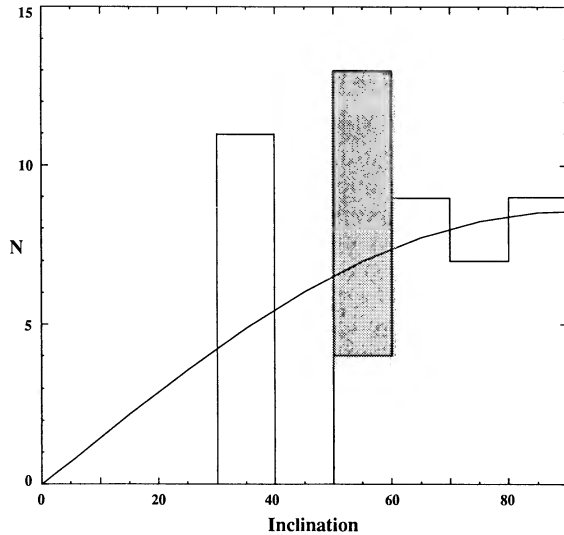


FIG. 3.—Histogram of the distribution of inclination angles for sources included in Table 1 and which have or are likely to have a circumstellar disk. Sources with a centrosymmetric pattern have been given an inclination of 30° . Sources (9) with an undetermined inclination have been attributed 52° (shaded area in the figure). The expected $\sin i$ distribution normalized to the total number of sources (49) is also plotted.

all been given an inclination of 30° . Another possible explanation for some of these sources is that they may not be surrounded by an optically thick disk, since single scattering only will also produce a centrosymmetric pattern. For the present purpose, we assume that all these sources have indeed an optically thick disk, which is probably true for most of them. In addition, nine sources (W3 IRS 1-2, L1551 NE, XZ Tau, VLA 1/HH 1-2, NGC 2071 IR, NGC 6334 IRS V, M 8 Hourglass, S140 [GL 2889], and LkH α 225) have been given the most probable value, $51^\circ.7$, since no good estimate of inclination could be found for reasons given in the notes to Tables 1 and 2. The distribution in Figure 3 is compatible with the expected $\sin i$ distribution for randomly distributed disk inclinations (see e.g., Bernacca 1970).

Weaver (1987) used the standard $L = 4\pi\sigma R^2 T^4$ relation to evaluate the inclination for a different set of T Tauri stars for which both the rotation period and $v \sin i$ were known. As he realized and as discussed in more detail by Hartmann and Stauffer (1989), one should take care when using this method because only the stellar luminosity must be used; the contributions from the disk and the boundary layer have to be subtracted from the observed bolometric luminosity. Neglecting that treatment leads to an anomalous distribution (Weaver 1987).

b) Inclination Angles

There have been very few estimations of the inclination angle of disks around the objects included in Table 1 so far. These estimations have been made in models aimed at explaining the energy distribution of young stellar objects (Adams, Lada, and Shu 1987; Kenyon and Hartmann 1987; Bertout, Basri, and Bouvier 1988; Basri and Bertout 1989). Adams, Lada, and Shu (1987) have assumed a viewing angle of 45° for most of the objects they considered because in their model, the emergent spectral energy distribution is not very sensitive on i , provided the disk is not seen edge-on. In their list, there is only

one object¹ in common with those given in Table 1, L1551 IRS 5, for which they give 70° based on the radial and tangential velocities of the associated Herbig-Haro objects. In Table 2, we derived $>80^\circ$ from a direct comparison of theoretical and observed polarization maps, or $\approx 81^\circ$ from the ratio of the disk axes. Given the uncertainties ($\pm 5^\circ$ from the polarization maps), the agreement is satisfactory.

Bertout, Basri, and Bouvier (1988) give inclination values for nine T Tauri stars, from fitting the observations from the UV to the mid-infrared with a computed energy distribution which takes into account the contributions of the stellar photosphere, the disk, and the boundary layer between disk and star. They claim an error of $\pm 10^\circ$ with their method. Finally, Basri and Bertout (1989) refined their energy distribution model, taking into account the possibility of optically thin emission from the boundary layer and obtained inclination values for 11 T Tauri stars, most of them being the same stars as studied by Bertout, Basri, and Bouvier (1988). They also mentioned that their solution is not unique, and that a different inclination can very often yield a good fit by changing the other parameters. Therefore, it is well advisable to have an independent knowledge of some of the parameters, in particular those which characterize the star itself. As an example of such an independent estimate, Bouvier and Bertout (1988) derived from a spot model, not the value of i , but a constraint on it, by explaining the rotational modulation of the T Tauri star DF Tau: $40^\circ \leq i \leq 90^\circ$. However, none of the stars in these papers are in common with those in Table 1.

Kenyon and Hartmann (1987), in their models of T Tauri and FU Orionis stars, report that the inclination is not well determined because it depends² rather critically on the extinction value used in the model. The extinction is at best poorly known, if at all.³ However, there are again no objects in common with those in Table 1.

Only one object listed in Table 2, HL Tau, has an inclination determined by another method. An infrared color map by Monin *et al.* (1989) led them to an inclination of $67^\circ \pm 7^\circ$, which is compatible with our value. However, they shifted the images so that the peak in the isophotes in the two filters coincide, which is not necessarily true, as they mentioned. In fact, our model predicts that the emission peaks should *not* coincide in many cases (see § Vd). This means that their value of inclination is really a lower limit to the inclination, since not recentering the images could increase the color gradient in their map.

c) Disk Sizes

We now compare the sizes of disks which we have determined in Table 2 with those given in the literature. From the angular sizes in Table 2, assuming typical distances of the order of 140 to 900 pc, the linear sizes are mostly from $\approx 10^3$ to $\approx \text{few} \times 10^4$ AU. These values indicate the sizes of the optically thick part of the disks at the wavelengths at which the

¹ This is one of the exceptions for which they estimated a value for the inclination.

² The point about the uniqueness of the solution was discussed further by Basri and Bertout (1989), as mentioned above.

³ All estimates of extinction (A_V) for stars surrounded by circumstellar material should take into account the fact that the light reaching the observer is in fact direct light extinguished by matter directly in front of the star *plus* light scattered by the circumstellar material in the observer's direction. This is not easily done and is almost always ignored in estimates of A_V , even though it has a significant impact on the results.

observations were made. They should be reliable since they are obtained directly from the observations, without relying on a model. In cases where the area of aligned vectors extends to the edge of the map, the sizes given should be taken as lower bounds.

On the other hand, the disks required to explain the spectral energy distributions are on the order of $\approx 10^1$ to $\approx 10^3$ AU (Adams, Lada, and Shu 1988; Bertout, Basri, and Bouvier 1988; Beckwith *et al.* 1989). In these models, increasing the disk radius increases the emission in the far-infrared (Bertout, Basri, and Bouvier 1988), however, since the radiation emitted by the grains in the far-infrared has so far not been included, one may say that the disk radius is not well determined by these models. Even at mm wavelengths, the disk radius is still only loosely constrained from spectral fits to the data, according to Beckwith *et al.* (1989) who used a radius of 100 AU to fit most of their data. The disk sizes determined from polarization maps are nevertheless on the high side compared to the sizes from models to explain the energy distribution. However, we caution here against an observational bias, namely that the objects in Table 1 have been chosen *because* they have extended nebulosities around them which cover most of the CCD detectors used for the observations. This gives a sample biased toward more massive objects. The models computed to account for the energy distribution have been aimed mostly at the less massive T Tauri stars. Therefore, a difference in disk size is to be expected.

One object, HL Tau, can be compared since it was considered by Adams, Lada, and Shu (1988) and has been mapped polarimetrically. Adams, Lada, and Shu (1988) found 100 AU as the *minimum* disk radius which fits the observed energy distribution. The $7''$ size measured from the polarization map gives a diameter of $\approx 10^3$ AU at a distance of 140 pc to the Taurus cloud. Given the uncertainties, these values are not incompatible with each other.

d) Position of the Emission Peak

A consequence of our model of optically thick circumstellar disks is that the star may not always be seen directly. This is the case for highly inclined disks, since the thickness of the disk is usually not negligible. Hence, what we think is the star, in many cases is not the star itself, but rather a "reflection" of the star on the nearby disk. We can usually tell if this is the case if the star is highly polarized. Two good examples of this phenomenon are HL Tau and R Mon. As a result, the maximum brightness in the isophote maps do not necessarily coincide at

different wavelengths. The longer wavelengths should give a better position of the central object, since the optical depth decreases with increasing wavelength.

VI. CONCLUSIONS

We have argued that dichroic extinction by aligned grains cannot explain polarization observations of young stars satisfactorily. Instead, we propose a model in which multiple scattering in optically thick disks, and single scattering in bipolar lobes explain the observed linear polarization maps *and* all other polarization properties of these stars. According to this later interpretation, we have presented a method for finding the size of optically thick disks around young stellar objects and for determining their inclination to our line of sight.

By comparing the observed polarization maps with computed maps which take single and double scattering into account, we have obtained inclination angles for more than 20 young stellar objects which show a pattern of aligned linear polarization vectors. The other objects which show a centrosymmetric pattern can be explained in one of two ways: (1) they have an optically thick disk with an inclination $\leq 55^\circ$ or (2) they are surrounded by nebular material with small optical depth so that single scattering only occurs. The distribution of inclination angles is compatible with the expected statistical distribution.

Unfortunately, there are not enough objects for which inclination angles have been obtained by other means to make a significant comparison. But the method presented above should in fact be more reliable than models aimed at explaining the energy distribution since in these models, the inclination is sensitive to the extinction required, which in turn is poorly known.

The sizes derived from the polarization maps appear larger than those required to explain the energy distribution, but this may be due mostly to an observational bias in favor of more massive stars and probably more massive and bigger disks. Observations of lower mass stars with smaller disks at high-spatial resolution is required to test this assumption.

Finally, a consequence of optically thick disks seen at high inclinations is that the peak in the isophote maps are not expected to coincide at different wavelengths, the longer wavelengths being closer to the central source.

We are grateful to the Natural Sciences and Engineering Research Council (NSERC) of Canada for financial assistance.

REFERENCES

- Adams, F., Lada, C. J., and Shu, F. 1987, *Ap. J.*, **312**, 788.
 ———, 1988, *Ap. J.*, **326**, 865.
 Aspin, C. 1988, in *Proc. Vatican Observatory Conf. on Polarized Radiation of Circumstellar Origin*, ed. G. V. Coyne, S. J., A. M. Magalhães, A. F. J. Moffat, R. E. Schulte-Ladbeck, S. Tapia, and D. T. Wickramasinghe (Vatican: Vatican Press), p. 693.
 Aspin, C., and McLean, I. S. 1984, *Astr. Ap.*, **134**, 333.
 Aspin, C., McLean, I. S., and Coyne, G. V. 1985, *Astr. Ap.*, **149**, 158.
 Aspin, C., McLean, I. S., and McCaughrean, M. J. 1985, *Astr. Ap.*, **144**, 220.
 Aspin, C., McLean, I. S., Schwarz, H. E., and McCaughrean, M. J. 1989, *Astr. Ap.*, **221**, 100.
 Basri, G., and Bertout, J. 1989, *Ap. J.*, **341**, 340.
 Bastien, P. 1985, *Ap. J. Suppl.*, **59**, 277.
 ———, 1987, *Ap. J.*, **317**, 231.
 ———, 1988a, in *NATO Advanced Study Institute, Galactic and Extragalactic Star Formation*, ed. P. Pudritz and M. Fich (Dordrecht: Kluwer), p. 303.
 ———, 1988b, in *Proc. Vatican Observatory Conf. on Polarized Radiation of Circumstellar Origin*, ed. G. V. Coyne, S. J., A. M. Magalhães, A. F. J. Moffat, R. E. Schulte-Ladbeck, S. Tapia, and D. T. Wickramasinghe (Vatican: Vatican Press), p. 541.
 Bastien, P., and Ménard, F. 1988, *Ap. J.*, **326**, 334 (BM).
 Bastien, P., Robert, C., and Nadeau, R. 1989, *Ap. J.*, **339**, 1089.
 Beckwith, S. V. W., Sargent, A. I., Chini, R. S., and Güsten, R. 1989, preprint.
 Bernacca, P. L. 1970, in *Stellar Rotation*, ed. A. Slettebak (Dordrecht: Reidel), p. 227.
 Bertout, C., Basri, G., and Bouvier, J. 1988, *Ap. J.*, **330**, 350.
 Bouvier, J., and Bertout, C. 1988, *Astr. Ap.*, **206**, 375.
 Burns, M. S., Hayward, T. L., Thronson, H. A., Jr., and Johnson, P. E. 1989, *A.J.*, **98**, 659.
 Castelaz, M. W., Hackwell, J. A., Grasdalen, G. L., Gehr, R. D., and Gullixson, C. 1985, *Ap. J.*, **290**, 261.
 Draper, P. W., Warren-Smith, R. F., and Scarrott, S. M. 1985a, *M.N.R.A.S.*, **212**, 1P.
 ———, 1985b, *M.N.R.A.S.*, **212**, 5P.
 ———, 1985c, *M.N.R.A.S.*, **216**, 7P.
 Drissen, L., Bastien, P., and St.-Louis, N. 1989, *A.J.*, **97**, 814.
 Gething, M. R., Warren-Smith, R. F., Scarrott, S. M., and Bingham, R. G. 1982, *M.N.R.A.S.*, **198**, 881.
 Gledhill, T. M., Warren-Smith, R. F., and Scarrott, S. M. 1986, *M.N.R.A.S.*, **223**, 867.
 ———, 1987, *M.N.R.A.S.*, **229**, 643.
 Gledhill, T. M., and Scarrott, S. M. 1989, *M.N.R.A.S.*, **236**, 153.

- Hartmann, L., and Stauffer, J. R. 1989, *A.J.*, **97**, 873.
 Heckert, P. A., and Zeilik, M. II. 1983, *M.N.R.A.S.*, **202**, 531.
 ———. 1984, *A.J.*, **89**, 1379.
 Hodapp, K.-W. 1984, *Astr. Ap.*, **141**, 255.
 Hough, J. H., Bailey, J., Cunningham, E. C., McCall, A., and Axon, D. J. 1981, *M.N.R.A.S.*, **195**, 429.
 Hough, J. H., *et al.* 1986, *M.N.R.A.S.*, **222**, 629.
 Joyce, R. R., and Simon, T. 1986, *A.J.*, **91**, 113.
 Kenyon, S. J., and Hartmann, L. 1987, *Ap. J.*, **323**, 714.
 King, D. J., Scarrott, S. M., and Taylor, K. M. R. 1983, *M.N.R.A.S.*, **202**, 1087.
 Lacasse, M. G. 1983, Ph.D. thesis, University of Rochester.
 Lacasse, M. G., Boyle, D., Levreault, R., Pipher, J. L., and Sharpless, S. 1981, *Astr. Ap.*, **104**, 57.
 Lenzen, R. 1987a, *Astr. Ap.*, **173**, 124.
 ———. 1987b, in *IAU Symposium 122, Circumstellar Matter*, ed. I. Appenzeller and C. Jordan (Dordrecht: Reidel), p. 127.
 Lenzen, R., Hodapp, K. W., and Solf, J. 1984, *Astr. Ap.*, **137**, 202.
 McLean, I. S., *et al.* 1987, *M.N.R.A.S.*, **225**, 393.
 Ménard, F. 1989, Ph.D. thesis, Université de Montréal.
 Ménard, F., and Bastien, P. 1987, in *IAU Symposium 122, Circumstellar Matter*, ed. I. Appenzeller and C. Jordan (Dordrecht: Reidel), p. 133.
 ———. 1990, in preparation.
 Ménard, F., Bastien, P., and Robert, C. 1988, *Ap. J.*, **335**, 290.
 Mestel, L., and Paris, R. B. 1984, *Astr. Ap.*, **136**, 98.
 Monin, J.-L., Pudritz, R. E., Rouan, D., and Lacombe, F. 1989, *Astr. Ap.*, **215**, L1.
 Nagata, T., *et al.* 1987, in *IAU Symposium 115, Star-Forming Regions*, ed. M. Peimbert and J. Jugaku (Dordrecht: Reidel), p. 374.
 Nadeau, R., and Bastien, P. 1986, *Ap. J. (Letters)*, **307**, L5.
 Notni, P. 1985, *Astr. Nach.*, **306**, 265.
 Redman, R. O., Kuiper, T. B. H., Lorre, J. J., and Gunn, J. E. 1986, *Ap. J.*, **303**, 300.
 Rolph, C. P., and Scarrott, S. M. 1988, *M.N.R.A.S.*, **234**, 719.
 Scarrott, S. M. 1988a, *M.N.R.A.S.*, **231**, 39P.
 ———. 1988b, *M.N.R.A.S.*, **231**, 1055.
 Scarrott, S. M., Brosch, N., Ward-Thompson, D., and Warren-Smith, R. F. 1986a, *M.N.R.A.S.*, **223**, 505.
 Scarrott, S. M., Draper, P. W., and Warren-Smith, R. F. 1989, *M.N.R.A.S.*, **237**, 621.
 Scarrott, S. M., Gledhill, T. M., and Warren-Smith, R. F. 1987a, *M.N.R.A.S.*, **227**, 701.
 ———. 1987b, *M.N.R.A.S.*, **227**, 1065.
 Scarrott, S. M., Gledhill, T. M., Warren-Smith, R. F., and Wolstencroft, R. D. 1987c, *M.N.R.A.S.*, **228**, 533.
 Scarrott, S. M., and Warren-Smith, R. F. 1988, *M.N.R.A.S.*, **232**, 725.
 Scarrott, S. M., Warren-Smith, R. F., Draper, P. W., Bruck, M. T., and Wolstencroft, R. D. 1987b, *M.N.R.A.S.*, **225**, 17P.
 Scarrott, S. M., Warren-Smith, R. F., Draper, P. W., and Gledhill, T. M. 1985, in *Cosmical Gas Dynamics*, ed. F. D. Kahn (Utrecht: VNU Science Press), p. 281.
 ———. 1986b, *Canadian J. Phys.*, **64**, 426.
 Scarrott, S. M., Warren-Smith, R. F., Wolstencroft, R. D., and Zinnecker, H. 1987a, *M.N.R.A.S.*, **228**, 827.
 Scarrott, S. M., and Wolstencroft, R. D. 1988, *M.N.R.A.S.*, **231**, 1019.
 Serkowski, K. 1973, in *IAU Symposium 52, Interstellar Dust and Related Topics*, ed. J. M. Greenberg and H. C. van de Hulst (Dordrecht: Reidel), p. 145.
 Shirt, J. V., Warren-Smith, R. F., and Scarrott, S. M. 1983, *M.N.R.A.S.*, **204**, 1257.
 Stocke, J. J., Hartigan, P. M., Strom, S. E., Strom, K. M., Anderson, E. R., Hartmann, L. W., and Kenyon, S. J. 1988, *Ap. J. Suppl.*, **68**, 229.
 Strom, S. E., Strom, K. M., Grasdalen, G. L., Sellgren, K., Wolf, S., Morgan, J., Stocke, J., and Mundt, R. 1985, *A.J.*, **90**, 2281.
 Ward-Thomson, D., Warren-Smith, R. F., Scarrott, S. M., and Wolstencroft, R. D. 1985, *M.N.R.A.S.*, **215**, 537.
 Warren-Smith, R. F. 1987, *Quart. J.R.A.S.*, **18**, 298.
 Warren-Smith, R. F., Draper, P. W., and Scarrott, S. M. 1987a, *Ap. J.*, **315**, 500.
 ———. 1987b, *M.N.R.A.S.*, **227**, 749.
 ———. 1987c, in *IAU Symposium 122, Circumstellar Matter*, ed. I. Appenzeller and C. Jordan (Dordrecht: Reidel), p. 129.
 Warren-Smith, R. F., Gledhill, T. M., and Scarrott, S. M. 1985, *M.N.R.A.S.*, **215**, 75.
 Warren-Smith, R. F., Scarrott, S. M., King, D. J., Taylor, K. N. R., Bingham, R. G., and Murdin, P. 1980, *M.N.R.A.S.*, **192**, 339.
 Warren-Smith, R. F., Scarrott, S. M., Murdin, P., and Bingham, R. G. 1979, *M.N.R.A.S.*, **187**, 761P.
 Weaver, W. B. 1987, *Ap. J. (Letters)*, **319**, L89.
 Werner, M. W., Dinerstein, H. L., and Capps, R. W. 1983, *Ap. J. (Letters)*, **265**, L13.
 Wolstencroft, R. D., Scarrott, S. M., and Menzies, J. 1988, in *IAU Symposium 135, Interstellar Dust*, ed. L. J. Allamandola and A. G. G. M. Tielens (Dordrecht: Reidel), in press.
 Wolstencroft, R. D., Scarrott, S. M., Warren-Smith, R. F., Walker, H. J., Reipurth, B., and Savage, A. 1986, *M.N.R.A.S.*, **218**, 1P.
 Wolstencroft, R. D., Scarrott, S. M., and Warren-Smith, R. F. 1987, *M.N.R.A.S.*, **228**, 805.
 Worden, S. P., and Grasdalen, G. L. 1974, *Astr. Ap.*, **34**, 37.
 Yamashita, T., *et al.* 1987a, *Pub. Astr. Soc. Japan*, **39**, 809.
 Yamashita, T., Sato, S., Nagata, T., Suzuki, H., Hough, J. H., McLean, I. S., Garden, R., and Gatley, I. 1987b, *Astr. Ap.*, **177**, 258.
 Yamashita, T., Sato, S., Tamura, M., Suzuki, H., Gatley, I., Hough, J. H., Mountain, C. M., and Moore, T. J. T. 1988, *M.N.R.A.S.*, **223**, 899.
 Zaritsky, D., Shaya, E. J., Scoville, N. Z., Sargent, A. I., and Tyler, D. 1987, *A.J.*, **93**, 1514.

PIERRE BASTIEN: Département de physique, Université de Montréal, B.P. 6128, Succ. A, Montréal, Québec, Canada H3C 3J7

FRANÇOIS MÉNARD: Institut d'Astrophysique de Paris, 98bis boul. Arago, 75014 Paris, France